Available online at www.sciencedirect.com
ScienceDirect
International Journal of Multiphase Flow 33 (2007) 1186–1204
International Journal of Multiphase Flow
www.elsevier.com/locate/ijmulflow

Stability of a viscous liquid film flowing down a periodic surface

Yu.Ya. Trifonov *

Institute of Thermophysics, Siberian Branch of Russian Academy of Sciences, Novosibirsk 630090, Russia

Received 16 February 2007; received in revised form 18 April 2007

Abstract

The paper is devoted to a theoretical analysis of linear stability of the viscous liquid film flowing down a wavy surface. The study is based on the Navier–Stokes equations in their full statement. The developed numerical algorithm allows us to obtain pioneer results in the stability of the film flow down a corrugated surface without asymptotic approximations in a wide range over Reynolds and Kapitsa's numbers. It is shown that in the case of moderate Reynolds numbers there is a region of the corrugation parameters (amplitude and period) where all disturbances decay in time and the wall corrugation demonstrates a stabilizing effect. At the same time, there exist corrugation parameters at which the steady-state solution is unstable with respect to perturbations of the same period as the period of corrugation. In this case the waveless solution cannot be observed in reality and the wall corrugation demonstrates a destabilizing effect.

Keywords: Viscous liquid film flow; Wavy surface; Corrugation; Stability

1. Introduction

Theoretical studies of film flows began with the classical work of Nusselt (1916) where he obtained exact solutions for the Navier–Stokes equations for a thin viscous layer falling down a smooth vertical wall. A great number of works have been devoted to both linear and non-linear analysis of wave formation on a free surface of the flow and there are many reviews devoted to wavy films. The problem of non-linear waves in the film falling down a smooth surface has much in common with that of a viscous layer flow along a corrugated surface. In both cases the governing equations are significantly nonlinear, the free surface is unknown, the surface tension forces play a great role and there exists a spatial period. In spite of numerous applications of the problem to distillation processes (Fair and Bravo, 1990; DeSantos et al., 1991) and compact heat exchangers (Shah and Focke, 1988; Webb, 1994) there are few experimental (Zhao and Cerro, 1992; Negny et al., 2001a,b; Vlachogiannis and Bontozoglou, 2002) and theoretical studies of the film flows down a corrugated surface. Using perturbation theory, Wang (1981) investigated the flow along a sinusoidal surface with a corrugation amplitude that was small compared to the Nusselt's thickness. Kang and Chen (1995) generalized this approach on

* Tel.: +7 383 330 60 40; fax: +7 383 330 84 80.
E-mail address: trifonov@itp.nsc.ru

0301-9322/$ - see front matter © 2007 Elsevier Ltd. All rights reserved.
doi:10.1016/j.ijmultiphaseflow.2007.05.004

two-layers flowing down an inclined, slightly wavy surfaces. Using boundary-integral computational analysis, Pozrikidis (1988) considered a creeping flow over an inclined periodic surface when the interia forces were ignored. Shetty and Cerro (1993) developed asymptotic analysis of flow when the film thickness is much smaller than the amplitude of corrugation. Treating corrugation in a linear approximation, Bontozoglou and Papapolymerou (1997) examined resonant effects at finite Reynolds numbers. Numerical solution of Navier–Stokes equations was obtained by Trifonov (1998) at finite values of Reynolds number for the corrugation amplitude that is comparable with the Nusselt film thickness. Film flow over a wavy wall in cylindrical geometry was investigated numerically by Negny et al. (2001a,b) on base of the Navier–Stokes equations. Their investigations were restricted by thin films in compare with the corrugations parameters. Film flow down a three-dimensional corrugated surface (with both large ribs and small surface texture) was studied by Trifonov (2004) on base of the integral approach.

All theoretical works mentioned above dealt with a waveless film flow down a corrugated surface. It is well-known that there are waves on the surface of film flowing down a smooth surface. What are the waves in the case of film flow down a corrugated surface? This question was studied by Trifonov (2007) on base of integral approach and two-periodical nonlinear regimes of flowing were obtained. Using a perturbation analysis the linear stability of film flow over an inclined wavy surface was considered by Wierschem and Aksel (2003) and Wierschem et al. (2005). Their analysis was devoted to the long undulations when the liquid free surface follows the corrugations shape. The goal of the present work is to study stability of the film flow down a corrugated surface in frame of Navier–Stokes equations. We need to obtain parameters where the integral or asymptotic approaches are still valid to describe more complicated regimes of flow down a corrugated surface. There are very few works where the film flow with a wavy free surface is considered by use of the Navier–Stokes equations in their full statement. One of them was carried out by Chin et al. (1986) where they investigated linear stability of the Nusselt film flow over a smooth surface at large values of Reynolds number ($Re > 100$).

2. Governing equations

Using a rectangular coordinate system the flow of viscous incompressible liquid along a vertical corrugated surface is described by Navier–Stokes equations with the corresponding boundary conditions (see, for example, Trifonov, 1998):

$$\frac{\partial u}{\partial t}+u\frac{\partial u}{\partial x}+v\frac{\partial u}{\partial y}=-\frac{\partial P}{\partial x}+\frac{1}{\varepsilon Re}\left(3+\frac{\partial^2 u}{\partial y^2}+\varepsilon^2\frac{\partial^2 u}{\partial x^2}\right);$$

$$\varepsilon^2\left(\frac{\partial v}{\partial t}+u\frac{\partial v}{\partial x}+v\frac{\partial v}{\partial y}\right)=-\frac{\partial P}{\partial y}+\frac{\varepsilon}{Re}\left(\frac{\partial^2 v}{\partial y^2}+\varepsilon^2\frac{\partial^2 v}{\partial x^2}\right);\quad \frac{\partial u}{\partial x}+\frac{\partial v}{\partial y}=0;$$

$$u=v=0,\quad y=\frac{1}{\varepsilon_1}f(x);$$

$$\frac{\partial u}{\partial y}+\varepsilon^2\frac{\partial v}{\partial x}+4\varepsilon^2\frac{\partial v}{\partial y}\frac{\partial h}{\partial x}\frac{1}{1-\varepsilon^2\left(\frac{\partial h}{\partial x}\right)^2}=0,\quad y=h(x,t);$$

$$P=P_a+\frac{2\varepsilon}{Re}\frac{\partial v}{\partial y}\frac{1+\varepsilon^2\left(\frac{\partial h}{\partial x}\right)^2}{1-\varepsilon^2\left(\frac{\partial h}{\partial x}\right)^2}-\varepsilon^2 We\frac{\frac{\partial^2 h}{\partial x^2}}{\left[1+\varepsilon^2\left(\frac{\partial h}{\partial x}\right)^2\right]^{3/2}},\quad y=h(x,t);$$

$$v=\frac{\partial h}{\partial t}+u\frac{\partial h}{\partial x},\quad y=h(x,t).$$

Here u is the velocity component in the x-direction, v is the velocity in the y-direction, P is the pressure in the liquid, P_a is the atmospheric pressure, $f(x)$ is the wall surface shape, $h(x,t)$ is the instantaneous film free surface shape, $H(x,t)=h(x,t)-(1/\varepsilon_1)f(x)$ is the instantaneous local film thickness.

The equations are written in a non-dimensional form using scales as follows (dimensional variables are denoted by asterisk):

$$x=\frac{x^*}{L};\quad y=\frac{y^*}{H_0};\quad t=\frac{u_0t^*}{L};\quad u=\frac{u^*}{u_0};\quad v=\frac{v^*}{\varepsilon u_0};\quad P=\frac{P^*}{\rho u_0^2};\quad H=\frac{H^*}{H_0};\quad f=\frac{f^*}{A};\quad h=\frac{h^*}{H_0};$$

$$Re=\frac{u_0H_0}{\nu}=\frac{gH_0^3}{3\nu^2};\quad \varepsilon=\frac{H_0}{L};\quad \varepsilon_1=\frac{H_0}{A};\quad We=\frac{(3Fi)^{1/3}}{Re^{5/3}};\quad Fi=\frac{(\sigma/\rho)^3}{g\nu^4}.$$

Here ν is the kinematic viscosity; ρ is the liquid density; σ is the surface tension; A and L are the corrugations amplitude and period, respectively; Re is the Reynolds number; Fi is the film number.

The free surface shape is unknown beforehand. We use coordinates transformation $t_1=t$, $x_1=x$, $\eta=(y-f(x)/\varepsilon_1)/H(x,t)$ and the flow area becomes known: $x_1\in[0,1]$, $\eta\in[0,1]$. Using new variables the non-stationary equations can be written as follows (the low index '1' is omitted):

$$\frac{\partial u}{\partial t}+\eta_t\frac{\partial u}{\partial \eta}=-\frac{\partial P}{\partial x}-\eta_x\frac{\partial P}{\partial \eta}+\frac{1}{\varepsilon Re}\left[3+\eta_y^2\frac{\partial^2 u}{\partial \eta^2}+\varepsilon^2\left(\frac{\partial^2 u}{\partial x^2}+\eta_x^2\frac{\partial^2 u}{\partial \eta^2}+2\eta_x\frac{\partial^2 u}{\partial x\,\partial \eta}+(\eta_{x\xi}+\eta_x\eta_{x\eta})\frac{\partial u}{\partial \eta}\right)\right]$$
$$-\eta_y\frac{\partial uv}{\partial \eta}-\frac{\partial u^2}{\partial x}-\eta_x\frac{\partial u^2}{\partial \eta};\tag{1}$$

$$\varepsilon^2\left(\frac{\partial v}{\partial t}+\eta_t\frac{\partial v}{\partial \eta}\right)=-\eta_y\frac{\partial P}{\partial \eta}+\frac{\varepsilon}{Re}\left[\eta_y^2\frac{\partial^2 v}{\partial \eta^2}+\varepsilon^2\left(\frac{\partial^2 v}{\partial x^2}+\eta_x^2\frac{\partial^2 v}{\partial \eta^2}+2\eta_x\frac{\partial^2 v}{\partial x\,\partial \eta}+(\eta_{x\xi}+\eta_x\eta_{x\eta})\frac{\partial v}{\partial \eta}\right)\right]$$
$$-\varepsilon^2\left(\frac{\partial uv}{\partial x}+\eta_x\frac{\partial uv}{\partial \eta}+\eta_y\frac{\partial v^2}{\partial \eta}\right);\tag{2}$$

$$v(t,x,\eta)=-H(t,x)u(t,x,\eta)\eta_x-\frac{\partial}{\partial x}\left(H\int_0^{\eta}u(t,x,\eta')\,\mathrm{d}\eta'\right);\tag{3}$$

$$\frac{\partial H}{\partial t}+\frac{\partial}{\partial x}\left(H(t,x)\int_0^1 u(t,x,\eta')\,\mathrm{d}\eta'\right)=0;\tag{4}$$

$$u(t,x,\eta)=0,\quad \eta=0;\tag{5}$$

$$P-P_{\mathrm{a}}=\frac{2\varepsilon}{Re}\eta_y\frac{\partial v}{\partial \eta}\frac{1+\varepsilon^2\left(\frac{\partial H}{\partial x}+\frac{1}{\varepsilon_1}\frac{\mathrm{d}f}{\mathrm{d}x}\right)^2}{1-\varepsilon^2\left(\frac{\partial H}{\partial x}+\frac{1}{\varepsilon_1}\frac{\mathrm{d}f}{\mathrm{d}x}\right)^2}-\varepsilon^2We\frac{\frac{\partial^2 H}{\partial x^2}+\frac{1}{\varepsilon_1}\frac{\mathrm{d}^2 f}{\mathrm{d}x^2}}{\left[1+\varepsilon^2\left(\frac{\partial H}{\partial x}+\frac{1}{\varepsilon_1}\frac{\mathrm{d}f}{\mathrm{d}x}\right)^2\right]^{3/2}},\quad \eta=1;\tag{6}$$

$$\left[\frac{\partial u}{\partial \eta}+\varepsilon^2H\frac{\partial v}{\partial x}-\varepsilon^2\left(\frac{\partial H}{\partial x}+\frac{1}{\varepsilon_1}\frac{\mathrm{d}f}{\mathrm{d}x}\right)\frac{\partial v}{\partial \eta}\right]\left[1-\varepsilon^2\left(\frac{\partial H}{\partial x}+\frac{1}{\varepsilon_1}\frac{\mathrm{d}f}{\mathrm{d}x}\right)^2\right]+4\varepsilon^2\frac{\partial v}{\partial \eta}\left(\frac{\partial H}{\partial x}+\frac{1}{\varepsilon_1}\frac{\mathrm{d}f}{\mathrm{d}x}\right)=0,\quad \eta=1.\tag{7}$$

Here $\eta_t=-\eta(\partial H/\partial t)/H(t,x)$; $\eta_x=-(\eta\partial H/\partial x+(1/\varepsilon_1)\mathrm{d}f(x)/\mathrm{d}x)/H(t,x)$; $\eta_y=1/H$; $\eta_{x\eta}\equiv(\eta_x)_\eta=-(\partial H/\partial x)/H$; $\eta_{x\xi}\equiv(\eta_x)_x=-(\eta_x/H)\partial H/\partial x-(\eta\partial^2H/\partial x^2+(1/\varepsilon_1)\mathrm{d}^2f(x)/\mathrm{d}x^2)/H(t,x)$.

Let us explain that the Eq. (3) follows from the continuity equation in new variables $\partial v/\partial\eta+\partial(Hu)/\partial x+\partial(H\eta_x u)/\partial\eta=0$ after the integration from 0 to η and taking into account the no-slip conditions at the wall. Eq. (4) follows from the kinematic boundary condition and Eq. (3) at $\eta=1$.

We are interesting in the steady-state solutions of Eqs. (1)–(7) $(H_b(x),u_b(x,\eta),v_b(x,\eta),P_b(x,\eta))$ and in their stability. In the case of flow over a smooth wall $(A=0)$ there is the analytical solution (Nusselts's solution):

$$H_b^0(x)=1,\quad u_b^0(x,\eta)=1.5(2\eta-\eta^2),\quad v_b^0(x,\eta)=0,\quad P_b^0(x,\eta)=P_{\mathrm{a}}.\tag{8}$$

Numerical methods should be involved to get the steady-state solutions at finite values of the corrugation amplitude. There are four independent parameters in the Eqs. (1)–(7) $\varepsilon,\varepsilon_1,Fi,Re$ and a function describing the wall configuration $f(x)$. We will use $L/\sqrt{\sigma/\rho g}$, A/L, Re and Ka ($Ka\equiv Fi^{1/11}$ is the Kapitsa number) as the independent parameters and $f(x)=0.5(1-\cos(2\pi x))$ for the calculations below. It is easy to see that the equations parameters can be expressed through our independent parameters – $\varepsilon=(3Re)^{1/3}/[Ka^{11/6}L/(\sqrt{\sigma/\rho g})]$, $\varepsilon_1=\varepsilon/(A/L)$.

Eqs. (1)–(7) were computed numerically by use of the spectral method to obtain the steady-state solutions:

$$u_b(x,\eta) = \frac{1}{2}U_1(x) + \sum_{m=2}^{M} U_m(x)T_{m-1}(\eta_1), \quad \eta_1 = 2\eta - 1,$$

$$U_m(x) = U_m^0 + \sum_{\substack{n=-N/2+1 \\ n\neq 0}}^{N/2-1} U_m^n \exp(2\pi i n x), \quad (U_m^{-n})^* = U_m^n, \quad m = 1,\ldots,M.$$

Here $T_m(\eta_1)$ are Chebyshev polinomials and the 'star' superscript designates complex conjugation.

At $M(N-1)$ known values of harmonics U_m^n the film thickness $H_b(x)$ is unambiguously regenerated from Eq. (4) – $H_b(x) = 1/\int_0^1 u_b(x,\eta')\,d\eta'$, the velocity $v_b(x,\eta)$ – from Eq. (3), $P_b(x,\eta)$ – from Eqs. (2) and (6). The numerical algorithm starts with the specification of the initial approximation for harmonics U_m^n which are then improved by Newton's method from Eq. (1) transformed into (n,m)-space. The Jacoby matrix was calculated by use of the first order differential scheme. Taking into account the boundary conditions (5) and (7) we have $(M+2)(N-1)$ nonlinear algebraic equations to obtain $M(N-1)$ unknown values, i.e. the system is overdefined. This problem is related to the fact that the basis functions in spectral expansion do not satisfy boundary conditions. In the current paper, we discard $2(N-1)$ equations corresponding to the last two Chebyshev coefficients in the expansion of the Eq. (1). The results will be correct at a good enough accuracy of approximation of the function $u_b(x,\eta)$ – $\left|U_m^{N/2-1}\right|/\sup\left|U_m^n\right| < 10^{-3}$ at any m, and $\left|U_M^n\right|/\sup\left|U_m^n\right| < 10^{-3}$ at any n. During the calculations, the indicated conditions of approximation were provided by the corresponding increasing of numbers N and M from 8 to 256 and from 5 to 50, respectively, depending on the parameters.

3. Stability of the steady-state solutions

Substituting

$$H = H_b(x) + \widehat{H}(x)\exp(-\lambda t) + \text{C.C.}, \quad u = u_b(x,\eta) + \hat{u}(x,\eta)\exp(-\lambda t) + \text{C.C.},$$
$$v = v_b(x,\eta) + \hat{v}(x,\eta)\exp(-\lambda t) + \text{C.C.}, \quad P = P_b(x,\eta) + \widehat{P}(x,\eta)\exp(-\lambda t) + \text{C.C.},$$
$$\eta_x = \bar{\eta}_x + \hat{\eta}_x, \quad \eta_y = \bar{\eta}_y + \hat{\eta}_y, \quad \eta_t = \hat{\eta}_t, \quad \eta_{x\eta} = \bar{\eta}_{x\eta} + \hat{\eta}_{x\eta}, \quad \eta_{x\xi} = \bar{\eta}_{x\xi} + \hat{\eta}_{x\xi},$$
$$\hat{\eta}_x = -\bar{\eta}_x\frac{\widehat{H}}{H_b} - \frac{\eta}{H_b}\frac{d\widehat{H}}{dx}, \quad \hat{\eta}_y = -\bar{\eta}_y\frac{\widehat{H}}{H_b}, \quad \hat{\eta}_t = \frac{\lambda\eta\widehat{H}}{H_b},$$
$$\hat{\eta}_{x\eta} = -\bar{\eta}_{x\eta}\frac{\widehat{H}}{H_b} - \frac{1}{H_b}\frac{d\widehat{H}}{dx}, \quad \hat{\eta}_{x\xi} = -\bar{\eta}_{x\xi}\frac{\widehat{H}}{H_b} - \frac{1}{H_b}\left(\hat{\eta}_x\frac{dH_b}{dx} + \bar{\eta}_x\frac{d\widehat{H}}{dx} + \eta\frac{d^2\widehat{H}}{dx^2}\right)$$

into the system (1)–(7) and linearizing the resultant equations near the steady-state solution, we obtain a system of equations with periodic coefficients to find a spectrum of eigenvalues:

$$a_1^1(x)\widehat{H} + a_2^1(x)\frac{d\widehat{H}}{dx} + a_3^1(x)\int_0^1 \hat{u}\,d\eta' + a_4^1(x)\frac{d}{dx}\int_0^1 \hat{u}\,d\eta' = \lambda\widehat{H}; \tag{9}$$

$$a_1^2(x,\eta)\widehat{H} + a_2^2(x,\eta)\frac{d\widehat{H}}{dx} + a_3^2(x,\eta)\frac{d^2\widehat{H}}{dx^2} + a_4^2(x,\eta)\hat{u} + a_5^2(x,\eta)\frac{\partial\hat{u}}{\partial x}$$
$$+ a_6^2(x,\eta)\frac{\partial\hat{u}}{\partial\eta} + a_7^2\frac{\partial^2\hat{u}}{\partial x^2} + a_8^2(x,\eta)\frac{\partial^2\hat{u}}{\partial\eta^2} + a_9^2(x,\eta)\frac{\partial^2\hat{u}}{\partial x\,\partial\eta} + a_{10}^2(x,\eta)\hat{v}$$
$$+ a_{11}^2(x,\eta)\frac{\partial\hat{v}}{\partial\eta} + \frac{\partial\widehat{P}}{\partial x} + a_{12}^2(x,\eta)\frac{\partial\widehat{P}}{\partial\eta} = \lambda[b_1^2(x,\eta)\widehat{H} + \hat{u}]; \tag{10}$$

$$\hat{u} = 0, \quad \eta = 0; \tag{11}$$

$$a_1^4(x)\widehat{H} + a_2^4(x)\frac{d\widehat{H}}{dx} + a_3^4(x)\frac{\partial\hat{u}}{\partial\eta} + a_4^4(x)\frac{\partial\hat{v}}{\partial x} + a_5^4(x)\frac{\partial\hat{v}}{\partial\eta} = 0, \quad \eta = 1; \tag{12}$$

$$a_1^5(x,\eta)\widehat{H} + a_2^5(x,\eta)\frac{\mathrm{d}\widehat{H}}{\mathrm{d}x} + a_3^5(x,\eta)\hat{u} + a_4^5(x)\int_0^\eta \hat{u}\,\mathrm{d}\eta' + a_5^5(x)\frac{\partial}{\partial x}\int_0^\eta \hat{u}\,\mathrm{d}\eta' + \hat{v} = 0; \tag{13}$$

$$\begin{aligned} &a_1^6(x,\eta)\widehat{H} + a_2^6(x,\eta)\frac{\mathrm{d}\widehat{H}}{\mathrm{d}x} + a_3^6(x,\eta)\frac{\mathrm{d}^2\widehat{H}}{\mathrm{d}x^2} + \int_\eta^1 \left[a_4^6(x,\eta')\hat{u} + a_5^6(x,\eta')\frac{\partial\hat{u}}{\partial x}\right. \\ &\quad + a_6^6(x,\eta')\frac{\partial\hat{u}}{\partial\eta'} + a_7^6(x,\eta')\hat{v} + a_8^6(x,\eta')\frac{\partial\hat{v}}{\partial x} + a_9^6(x,\eta')\frac{\partial\hat{v}}{\partial\eta'} + a_{10}^6\frac{\partial^2\hat{v}}{\partial x^2} \\ &\quad \left. + a_{11}^6(x,\eta')\frac{\partial^2\hat{v}}{\partial\eta'^2} + a_{12}^6(x,\eta')\frac{\partial^2\hat{v}}{\partial x\,\partial\eta'}\right]\mathrm{d}\eta' + \frac{1}{H_b(x)}\widehat{P}(x,\eta)\Big|_{\eta=1} - \frac{\widehat{P}(x,\eta)}{H_b(x)} \\ &\quad = \lambda\left[b_1^6(x,\eta)\widehat{H} + \varepsilon^2\int_\eta^1 \hat{v}\,\mathrm{d}\eta'\right]; \end{aligned} \tag{14}$$

$$\widehat{P}(x,\eta)\Big|_{\eta=1} = a_1^7(x)\widehat{H} + a_2^7(x)\frac{\mathrm{d}\widehat{H}}{\mathrm{d}x} + a_3^7(x)\frac{\mathrm{d}^2\widehat{H}}{\mathrm{d}x^2} + a_4^7(x)\frac{\partial\hat{v}}{\partial\eta}\Big|_{\eta=1}.$$

Here C.C. designates value that is complex conjugate to the disturbance and the bar denotes value calculated at substitution of the steady-state solution. Coefficients a_j^i, b_j^i in Eqs. (9)–(14) are real functions and ones are expressed through the steady-state solution (see Appendix).

According to Floquet's theorem, the solutions of Eqs. (9)–(14) bounded in terms of the x-coordinate are presented as follows:

$$\begin{pmatrix} \widehat{H} \\ \hat{u} \\ \hat{v} \\ \widehat{P} \end{pmatrix} = \begin{pmatrix} \sum\limits_{n=-N/2+1}^{n=N/2-1} \widehat{H}_n \exp(2\pi\mathrm{i}nx) \\ \frac{1}{2}\sum\limits_{n=-N/2+1}^{n=N/2-1} \hat{u}_{1n}\exp(2\pi\mathrm{i}nx) + \sum\limits_{m=2}^{M} T_{m-1}(\eta_1)\sum\limits_{n=-N/2+1}^{n=N/2-1} \hat{u}_{mn}\exp(2\pi\mathrm{i}nx) \\ \frac{1}{2}\sum\limits_{n=-N/2+1}^{n=N/2-1} \hat{v}_{1n}\exp(2\pi\mathrm{i}nx) + \sum\limits_{m=2}^{M} T_{m-1}(\eta_1)\sum\limits_{n=-N/2+1}^{n=N/2-1} \hat{v}_{mn}\exp(2\pi\mathrm{i}nx) \\ \frac{1}{2}\sum\limits_{n=-N/2+1}^{n=N/2-1} \widehat{P}_{1n}\exp(2\pi\mathrm{i}nx) + \sum\limits_{m=2}^{M} T_{m-1}(\eta_1)\sum\limits_{n=-N/2+1}^{n=N/2-1} \widehat{P}_{mn}\exp(2\pi\mathrm{i}nx) \end{pmatrix} \exp(2\pi\mathrm{i}Qx).$$

Here Q is a real parameter varying from zero to unity $Q \in [0,1]$. After substitution into Eqs. (9)–(14) we have a generalized eigenvalue problem for complex matrixes:

$$A\hat{x} = \lambda B\hat{x}; \quad \hat{x} = \begin{pmatrix} \widehat{H}_n \\ \hat{u}_{mn} \\ \hat{v}_{mn} \\ \widehat{P}_{mn} \end{pmatrix}. \tag{15}$$

Matrixes A and B are of order $(3M+1)(N-1)$ and ones were computed numerically column by column varying unit vector of the disturbances. We discard $2(N-1)$ equations corresponding to the last two Chebyshev coefficients in the expansion of Eq. (10). Instead of them the boundary conditions (11) and (12) are used. To study stability of the solution $(H_b(x), u_b(x,\eta), v_b(x,\eta), P_b(x,\eta))$ we have to analyze $(3M+1)(N-1)$ eigenvalues for each value of the parameter $Q \in [0,1]$. The solution is stable if the real parts of all eigenvalues are greater than zero or equal to zero for all Q. Disturbances with $Q = 0$ should be distinguished. These disturbances have the same period as the basic solution. Instability with respect to this class of disturbances manifests itself in the fact that the steady-state viscous flow is impossible to observe in reality. Regimes unstable with respect to disturbances with finite values of Q can be observed until the disturbances will be developed.

4. Results of the calculations. Stability of the film flows down a smooth surface

Steady-state solution (8) was examined firstly regarding the stability and results are presented in Figs. 1 and 2 (here $\alpha_{\text{neut}} \equiv 2\pi H_0/\lambda^*_{\text{neut}}$, λ^*_{neut} is the dimensional period of neutral disturbance). The calculations were performed for three values of the Kapitza number $Ka = Fi^{1/11}$. First of them ($Ka = 10$) is close to the water film number or to the film number of liquid nitrogen on the saturation line at atmospheric pressure. Second and third values of Fi correspond to water-glycerol mixtures used by Alekseenko et al. (1992) in experiments on wavy film flow. Parameter L in this case has no physical meaning (only a scale) and in the equations we can use $L = H_0$ $(\varepsilon = 1, 1/\varepsilon_1 = 0)$ and $\lambda^* = H_0/Q$ is the disturbance dimensional period. Problem (15) in this case is simplified because the coefficients a_i^j in Eqs. (9)–(14) do not depend on the x-coordinate. At all values of the Reynolds number Re (at least up to 1000) and at $Q < Q_{\text{neut}}(Re, Fi^{1/11})$ spectrum of the eigenvalues of (15)

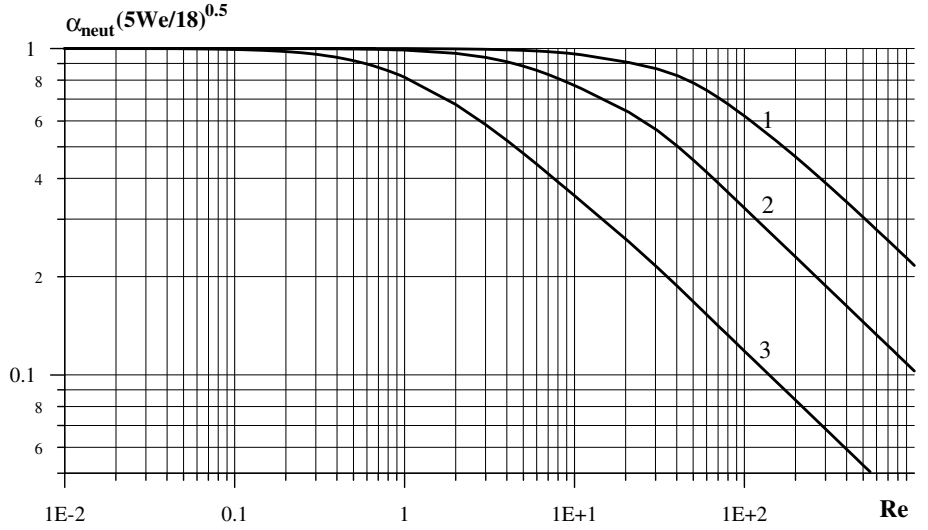

Fig. 1. Wave numbers of the neutral disturbances. Lines 1–3 correspond to the Navier–Stokes equations calculations at $Fi^{1/11} = 10$, 5 and 2, respectively. Result of Benjamin (1957) asymptotic approach is $\alpha_{\text{neut}}\sqrt{5We/18} = 1$ at all values of Re and $Fi^{1/11}$.

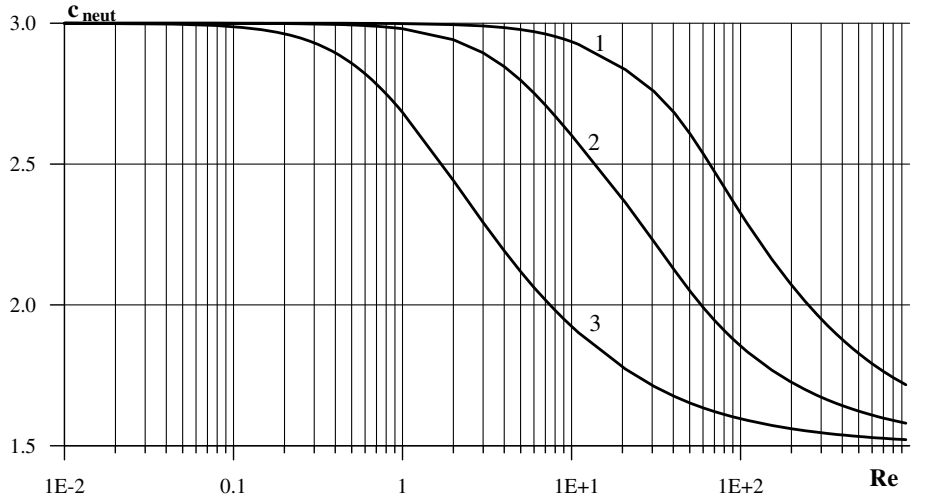

Fig. 2. Phase velocity of the neutral disturbances. Lines 1–3 correspond to the Navier–Stokes equations calculations at $Fi^{1/11} = 10$, 5 and 2, respectively. Result of Benjamin (1957) asymptotic approach is $c_{\text{neut}} = 3$ at all values of Re and $Fi^{1/11}$.

has a single unstable mode. Let us note that the number of Chebyshev polynomials M in the disturbances approximation was varied in a wide range (from 10 up to 50). Dependences presented in Figs. 1 and 2 were calculated at $M = 25$ (for all values of the Kapitsa and Reynolds numbers) and ones were not changed at further increasing of M.

At relatively small values of Re the dependences in Figs. 1 and 2 correspond to results of asymptotic approach (Benjamin, 1957; $(\alpha_{\text{neut}})_B\sqrt{5We/18} = 1$). Using definition of H_0 and We it is easy to see that $\lambda^*_{\text{neut}} \approx (\lambda^*_{\text{neut}})_B = 2\pi\sqrt{5\sigma/(6\rho g Re)}$ in this case and the neutral disturbance period decreases with the Reynolds number increasing (all modes with $\lambda^*_{\text{neut}} < \lambda^* < \infty$ are unstable). Phase velocity of the neutral disturbance is close to the double free surface velocity at these values of Re. Integral approach (see, for example, Alekseenko et al., 1992) gives $(\lambda^*_{\text{neut}})_I = 2\pi\sqrt{\sigma/(\rho g Re)}$ at all values of Re and Ka.

There is essential discrepancy between the predictions of the asymptotic or integral approaches and our results at moderate and large values of Re. The discrepancy increases with the film number decreasing. Let us not that the dependences in Fig. 1 demonstrate asymptotic straight line at large values of Re ($\alpha_{\text{neut}}\sqrt{5We/18} \sim 1/\sqrt{Re}$). Period of the neutral disturbance will depend only on the liquid physical properties at these values of Re – $\lambda^*_{\text{neut}} = C\sqrt{\sigma/\rho g}$, $C = C(Fi^{1/11})$, and one will not depend on the liquid flow rate. Phase

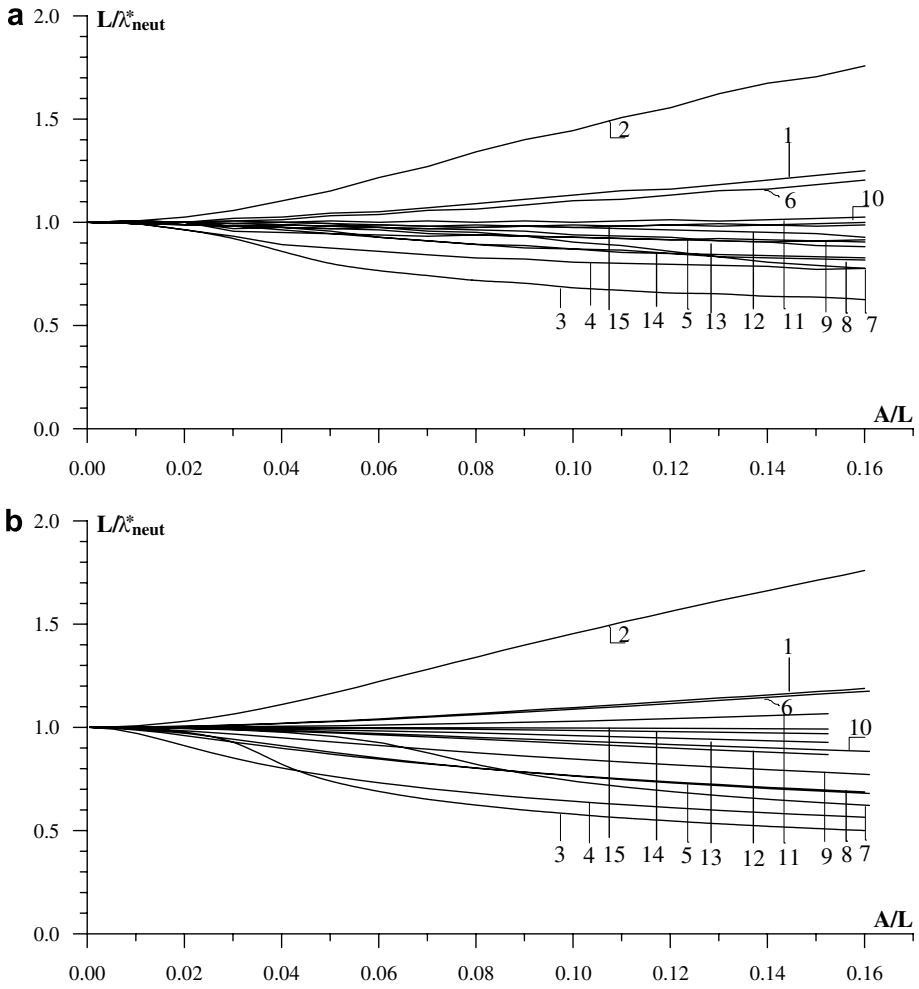

Fig. 3. Corrugations parameters (below the corresponding line) where the steady-state solution is stable with respect to disturbances of the same period ($Q = 0$): (a) corresponds to the Navier–Stokes equations ($\lambda^*_{\text{neut}}/H_0$ is presented in Fig. 1); (b) integral model ($\lambda^*_{\text{neut}}/H_0 = 2\pi\sqrt{We/3}$). Lines 1–5 correspond to $Fi^{1/11} = 10$ at $Re = 1$, 5, 10, 20 and 50, respectively; lines 6–10 – $Fi^{1/11} = 5$ at $Re = 1$, 5, 10, 20 and 50, respectively; lines 11–15 – $Fi^{1/11} = 2$ at $Re = 1$, 5, 10, 20 and 50, respectively.

velocity of the neutral disturbance is close to the free surface velocity at these values of Re. The last two conclusions are in agreement with the results of Chin et al. (1986) where they investigated linear stability of film flow over a smooth surface at large values of Reynolds number ($Re > 100$).

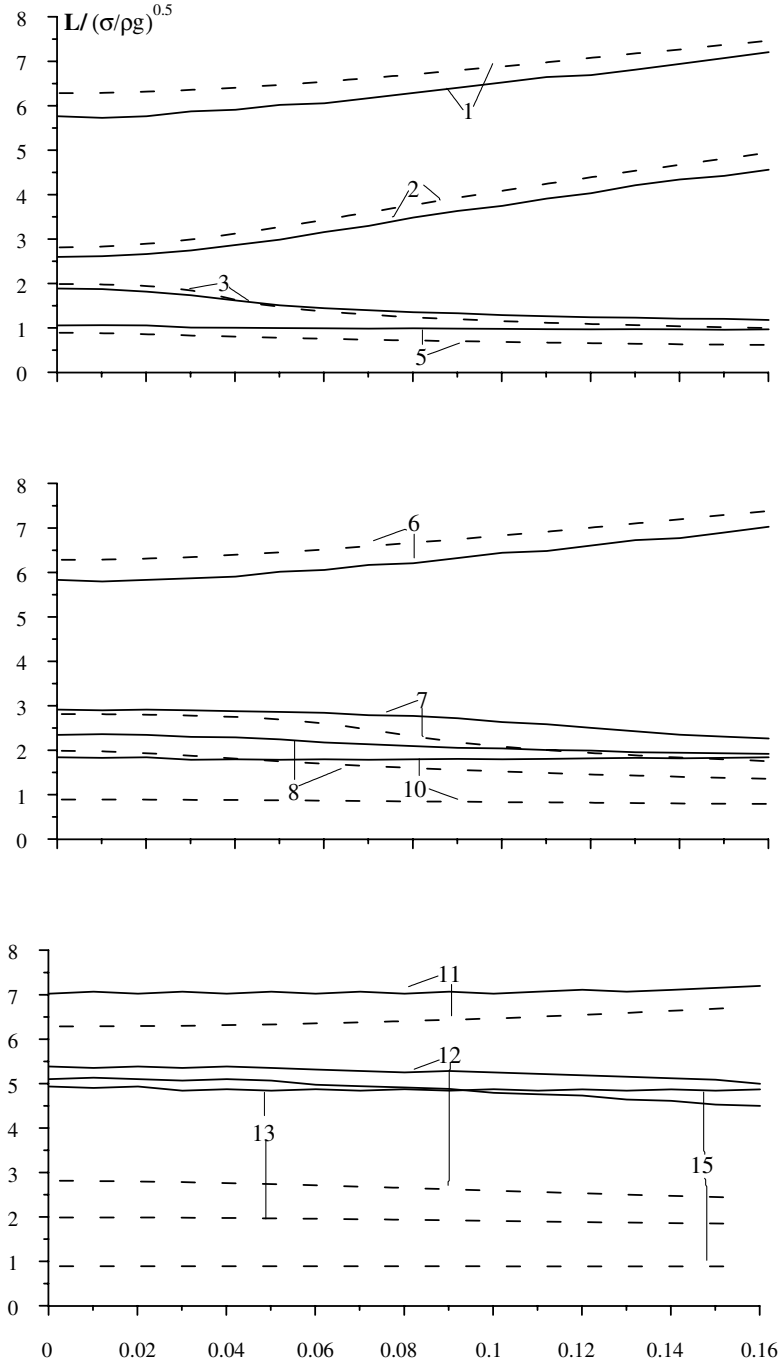

Fig. 4. Corrugations parameters (below the corresponding line) where the steady-state solution is stable with respect to disturbances of the same period ($Q = 0$); solid lines corresponds to the Navier–Stokes equations; dashed lines – integral model. The lines parameters are explained in caption of Fig. 3.

5. Results of the calculations. Stability of the film flows down a corrugated surface

Calculations of the steady-state regimes start at small values of the corrugation amplitude where we have initial guess (solution (8)) of the iteration procedure. Varying parameters the steady-state solutions were obtained and their stability was analyzed at wide range of $L/\sqrt{\sigma/\rho g}$ and A/L at three values of $Ka = Fi^{1/11}$ and for the values of $Re = 1$, 5, 10, 20 and 50.

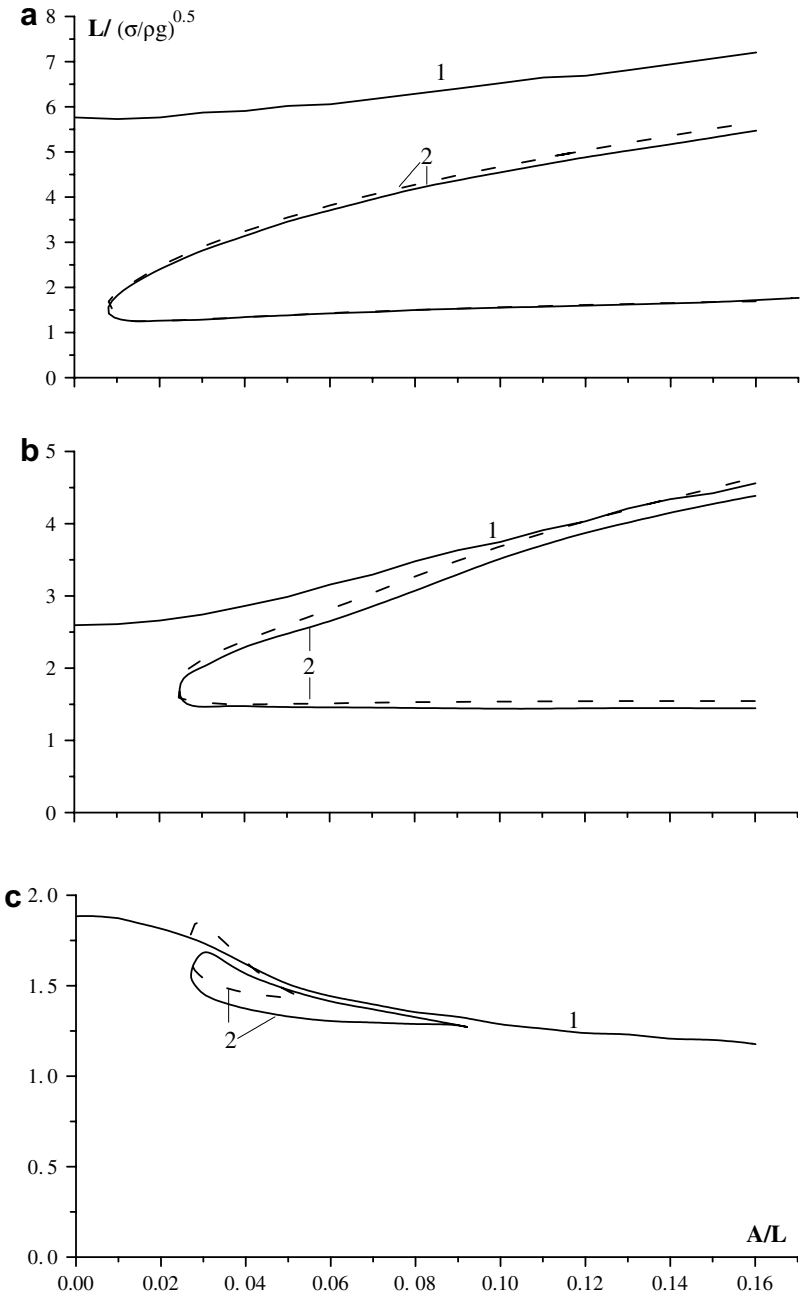

Fig. 5. Corrugations parameters where the steady-state solution is stable with respect to disturbances of the same period (below line 1) and ones where the solution is stable with respect to arbitrary disturbances $Q \in [0, 1]$ (inside region bounded by line 2). Solid lines corresponds to the Navier–Stokes equations; dashed lines – integral model. Value of $Fi^{1/11} = 10$: (a) corresponds to $Re = 1$; (b) $Re = 5$; (c) $Re = 10$.

Results of the stability study are presented in Figs. 3a and 4–7. The corresponding results of the integral approach obtained by Trifonov (2007) are shown in Figs. 3b and 4–6 as dashed lines. Figs. 8–11 demonstrate basic characteristics of the solutions of the Navier–Stokes equations at the parameters variation. Here $\langle H \rangle$ is the averaged local film thickness, $H_{\max}$ and $H_{\min}$ are the maximum and minimum of the local film thickness over a period, respectively. The contour lines of the streamline function $\Psi(x,\eta) = \int_0^\eta H(x)u_b(x,\eta')\,\mathrm{d}\eta'$ are

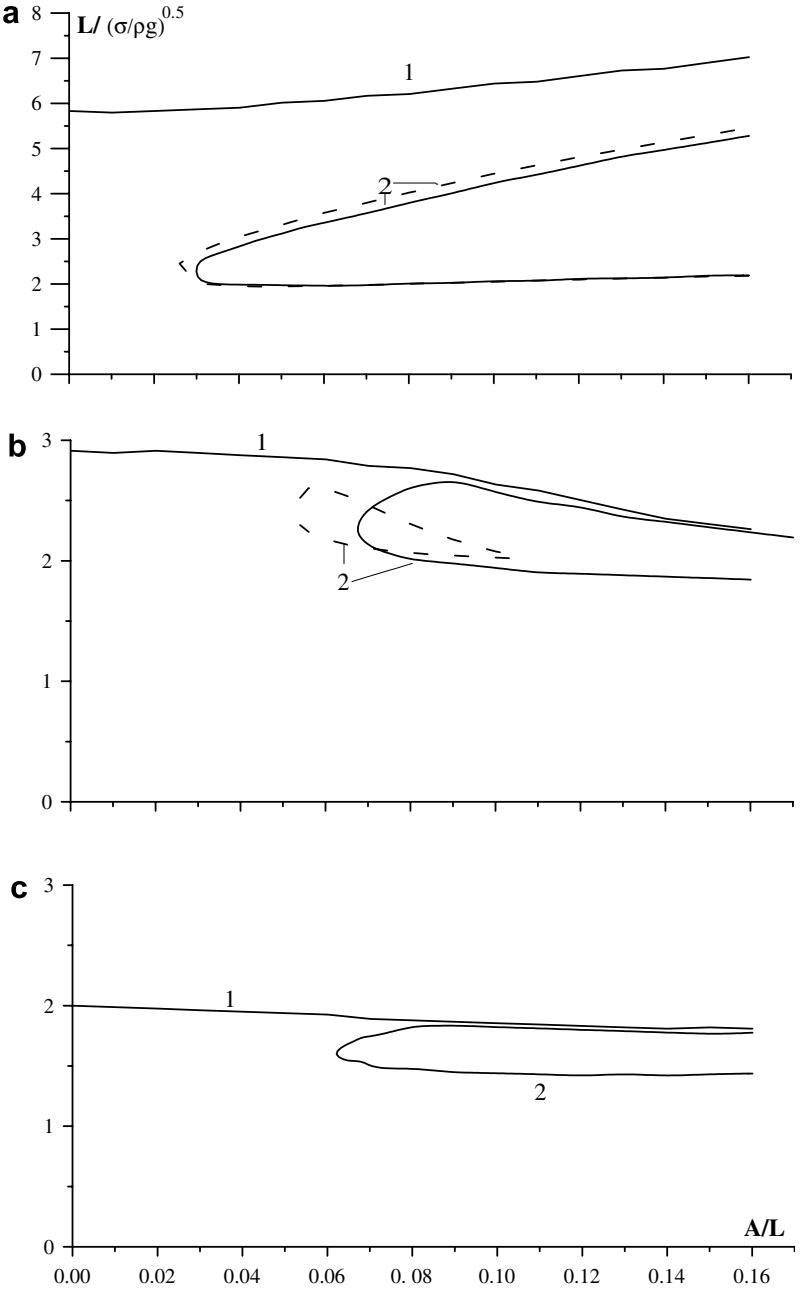

Fig. 6. Corrugations parameters where the steady-state solution is stable with respect to disturbances of the same period (below line 1) and ones where the solution is stable with respect to arbitrary disturbances $Q \in [0, 1]$ (inside region bounded by line 2). Solid lines corresponds to the Navier–Stokes equations; dashed lines – integral model. Value of $Fi^{1/11} = 5$: (a) corresponds to $Re = 1$; (b) $Re = 5$; (c) $Re = 20$, no region 2 in accordance with the integral approach.

shown in Fig. 12. In steady flow, the streamlines represent particle trajectories within the liquid. The wall and the free surface shapes are the low and upper bounds of the plot, respectively ($y/L = \varepsilon[f(x)/\varepsilon_1 + \eta H_b(x)]$). In Fig. 13, the corresponding streamline function of the integral approach and the free surface shape are presented for comparison.

There are real eigenvalues and pairs of the complex conjugate eigenvalues in spectrum of problem (15) at $Q = 0$. On lines 1–15 in Figs. 3 and 4 (or on line 1 in Figs. 5 and 6) the real part of one pair of complex

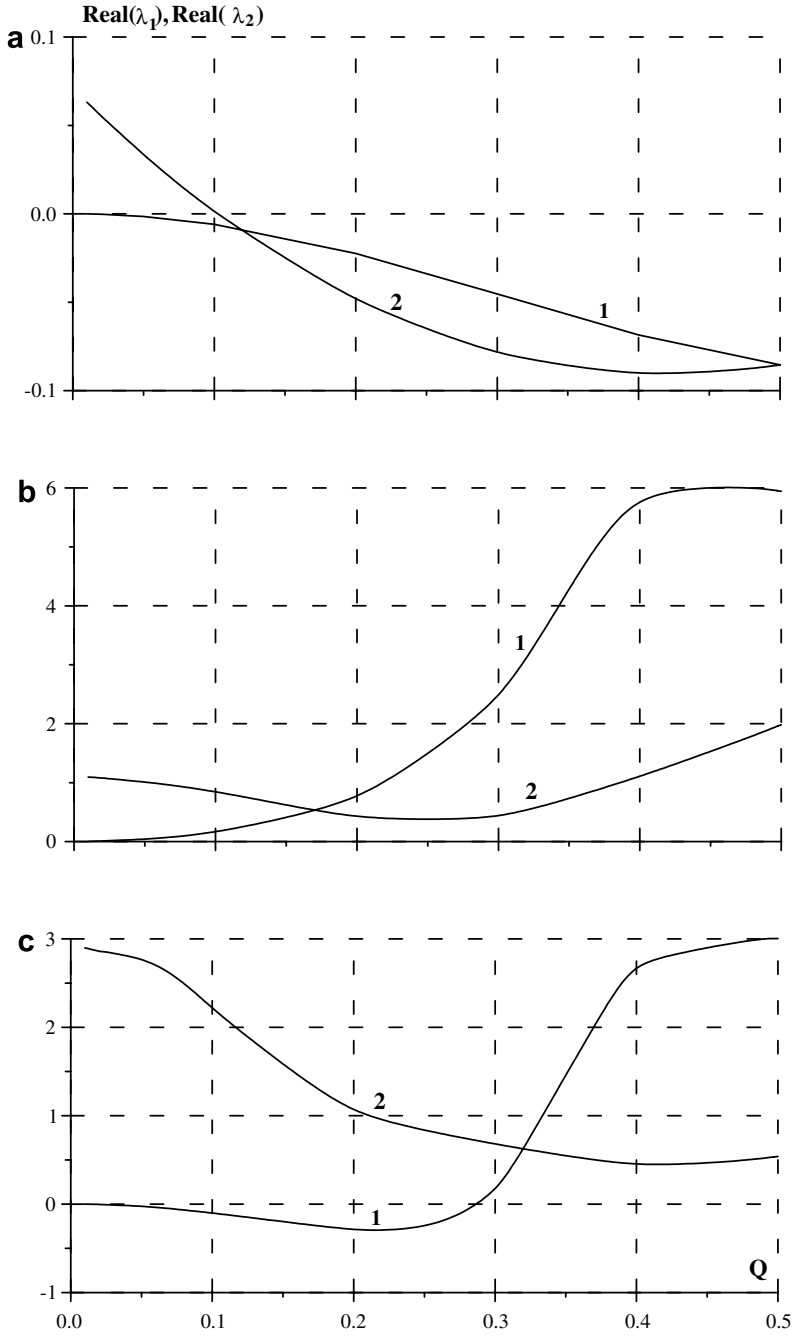

Fig. 7. Behaviour of the real parts of two eigenvalues as a function of parameter Q at different values of the corrugation period. The steady-state solution is stable if Real(λ) of all eigenvalues is positive at all values of $Q \in [0, 0.5]$. Values of $Fi^{1/11} = 10$, $Re = 5$, $A/L = 0.1$: (a) corresponds to $L/\sqrt{\sigma/\rho g} = 3.7$; (b) $L/\sqrt{\sigma/\rho g} = 2$; (c) $L/\sqrt{\sigma/\rho g} = 1$.

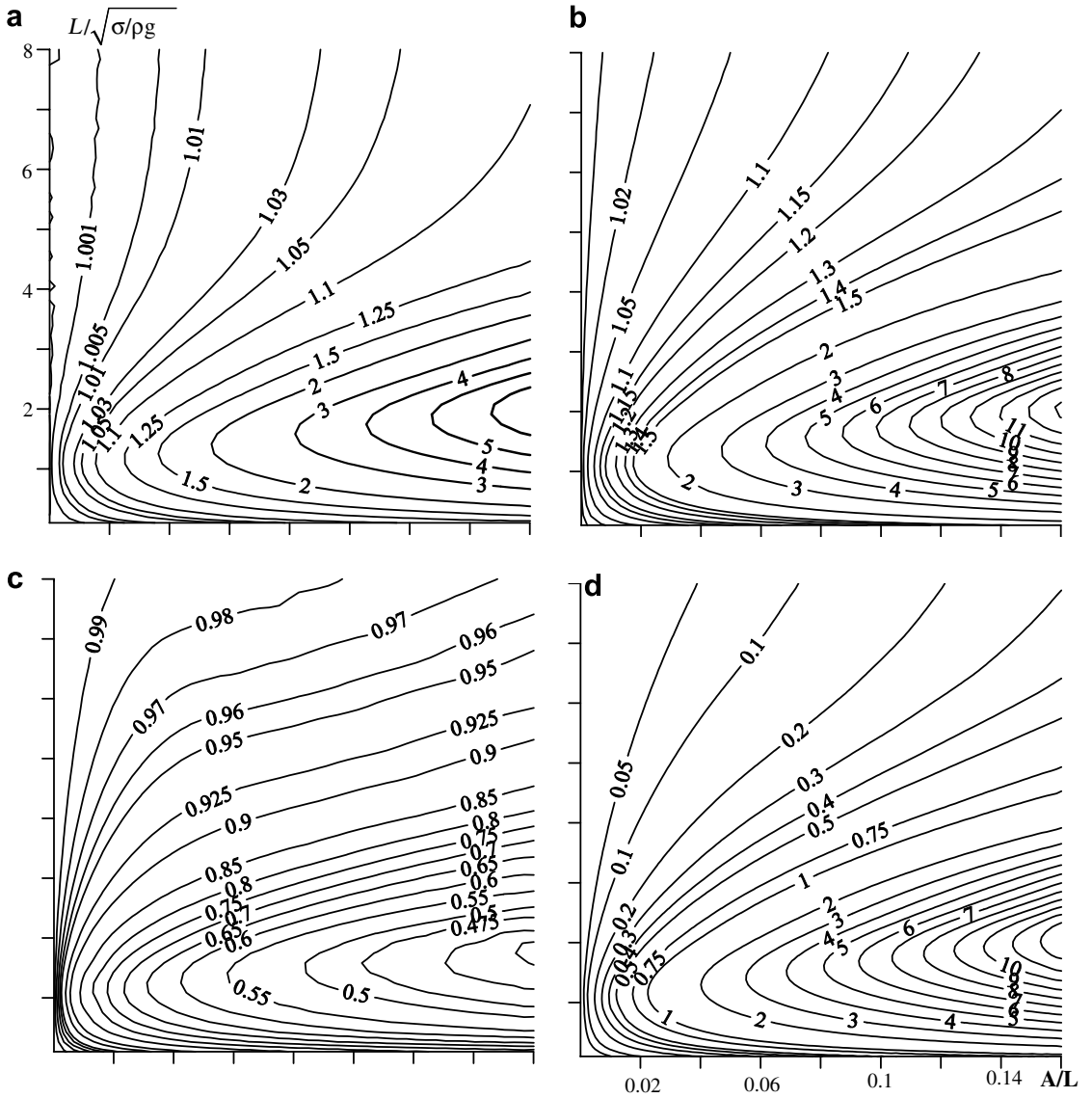

Fig. 8. Contour lines of basic characteristics of the steady-state solutions on the plane of the corrugation parameters. Values of $Fi^{1/11} = 10$, $Re = 1$: (a) corresponds to $\langle H \rangle$; (b) H_{max}; (c) H_{min}; (d) $(H_{max} - H_{min})$.

conjugate values goes through zero. Below these lines the solutions are stable with respect to disturbances with $Q = 0$. At these values of the corrugation and flow parameters the basic wavyless solution can be observed in experiments (at least over an initial part of the experimental channel) while the unstable disturbances with finite values of Q or the possible unstable three-dimensional disturbances will be developed. In experiments of Vlachogiannis and Bontozoglou (2002), devoted to the film flow over inclined corrugated channel they called this part of the flow as "free surface with static deformation". Above the lines 1–15 in Figs. 3 and 4 (or above line 1 in Figs. 5 and 6) the solutions are unstable with respect to disturbances with $Q = 0$ and the wavyless basic solution cannot be observed experimentally even on the initial part of the flow channel. Let us note that the value λ^*_{neut} (period of the neutral disturbance of the film flow down a smooth surface) used as a scale in Fig. 3a depends essentially on Re and Ka (see Fig. 1). Let us also note that the lines 1–15 in Fig. 3a are close enough to unity at all values of the corrugation amplitude and ones are close to the corresponding lines of the integral approach (Fig. 3b). Fig. 4 presents the same results using capillary constant as a scale of

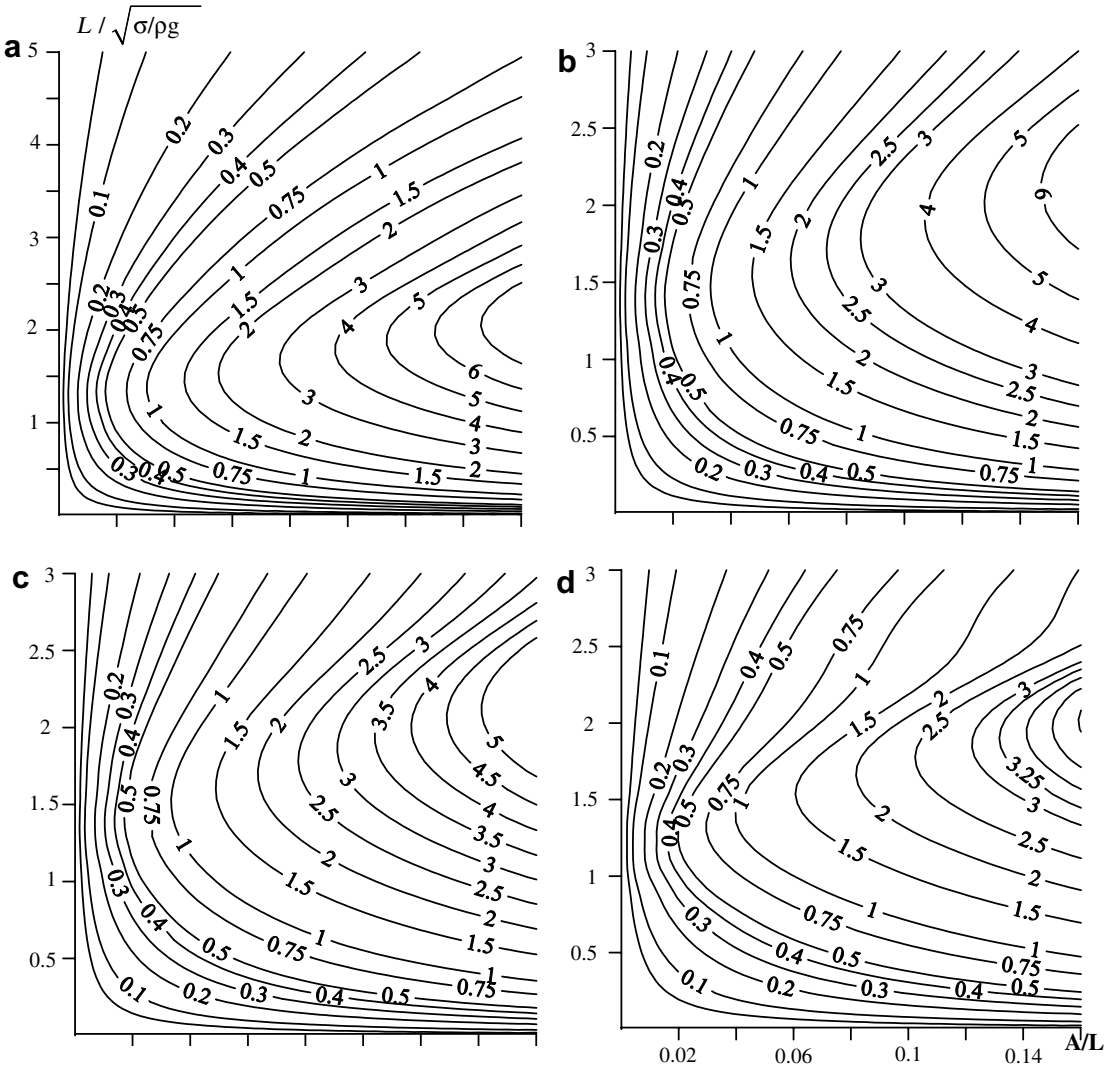

Fig. 9. Contour lines of $(H_{\max} - H_{\min})$ on the plane of the corrugation parameters. Values of $Fi^{1/11} = 10$: (a) corresponds to $Re = 5$; (b) $Re = 10$; (c) $Re = 20$; (d) $Re = 50$.

the corrugation period. Both the lines scattering and the difference from the integral approach are more essential in this system of non-dimensional parameters (due to essential dependence of λ^*_{neut} on Re and Ka). Nevertheless we will use $L/\sqrt{\sigma/\rho g}$ as a non-dimensional parameter for rest of the paper graphs due to more clear connection with the liquid physical property.

There are three different regimes of the film flowing over a wavy wall as it follows from Figs. 8–13. First of them is characterized by the free surface shape that follows the wall shape and one is realized at large values of $L/\sqrt{\sigma/\rho g}$. The value of $(H_{\max} - H_{\min})$ is relatively small for this type of flowing and $\langle H \rangle$ is close to one. Second regime of flowing is characterized both by the deformed free surface shape and by the existence of the area of "thick" film over the corrugation period resulting in an essential increasing of the value of $(H_{\max} - H_{\min})$. This type of flowing is realized at moderate values of $L/\sqrt{\sigma/\rho g}$. Third type of flowing is realized at small values of $L/\sqrt{\sigma/\rho g}$ and the film free surface is almost parallel to the x-axis for this regime. These three types of flowing exist at all values of Re and Ka considered in the paper. Comparison with the stability analysis results presented in Fig. 4 allows us to conclude that the first regime of flowing is unstable with respect to disturbances with $Q = 0$. Using a perturbation analysis the stability of the first type of flowing over the inclined

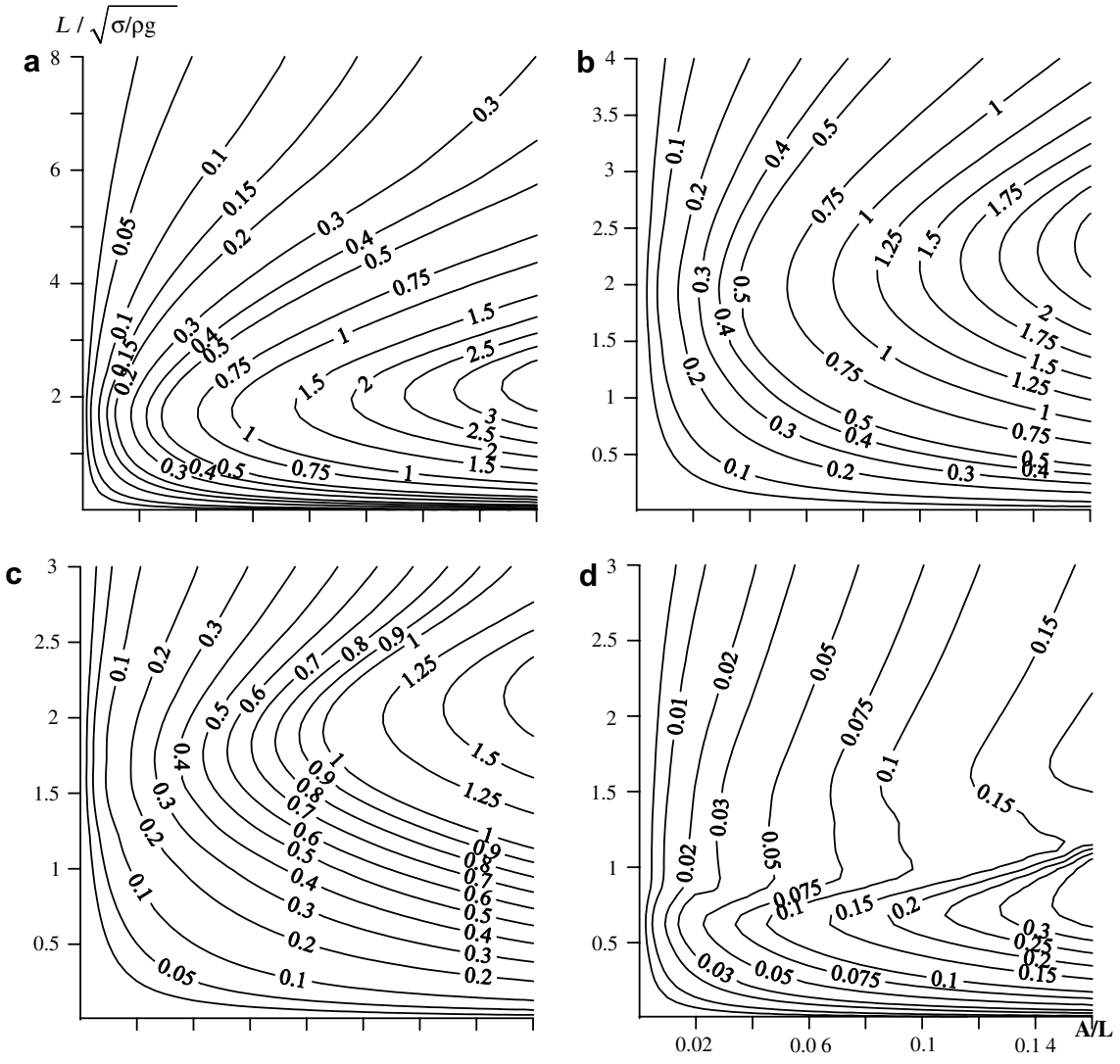

Fig. 10. Contour lines of $(H_{\max} - H_{\min})$ on the plane of the corrugation parameters. Values of $Fi^{1/11} = 5$: (a) corresponds to $Re = 1$; (b) $Re = 5$; (c) $Re = 20$; (d) $Re = 50$.

corrugated wall was considered by Wierschem and Aksel (2003) and Wierschem et al. (2005). They found that the critical Reynolds number for the onset of surface waves is higher than for a flat bottom but one is still zero for the flow down a vertical corrugated wall. We are going to analyze stability of the film flow over inclined wavy wall in nearest future based on the Navier–Stokes equations in their full statement. Now it is not possible to give comparison of our results with these papers conclusions.

Above, the stability with respect to disturbances of the same period as the period of corrugations was analyzed. This class of disturbances is very important but there are other disturbances which can be unstable. Time-evolution of any disturbance of our basic periodical regime can be presented through a set of two-periodical perturbations $(\widehat{H}(x), \hat{u}(x,\eta), \hat{v}(x,\eta), \widehat{P}(x,\eta)) \exp(-\lambda t) \exp(2\pi i Q x)$ in accordance with the Floquet's theorem. One of the perturbations periods is the period of corrugations and the second period is L/Q. For every value of $Q \in [0,1]$ we should analyze the spectrum of the eigenvalues of problem (15) to give answer regarding the stability. There are harmonics of period $L, L/2, \ldots, 2L/N$ in the Fourier expansion of $(\widehat{H}(x), \hat{u}(x,\eta), \hat{v}(x,\eta), \widehat{P}(x,\eta))$ and our stability analysis covers all types of disturbances with different wavelengths (equal, shorter and longer with respect to the wall period).

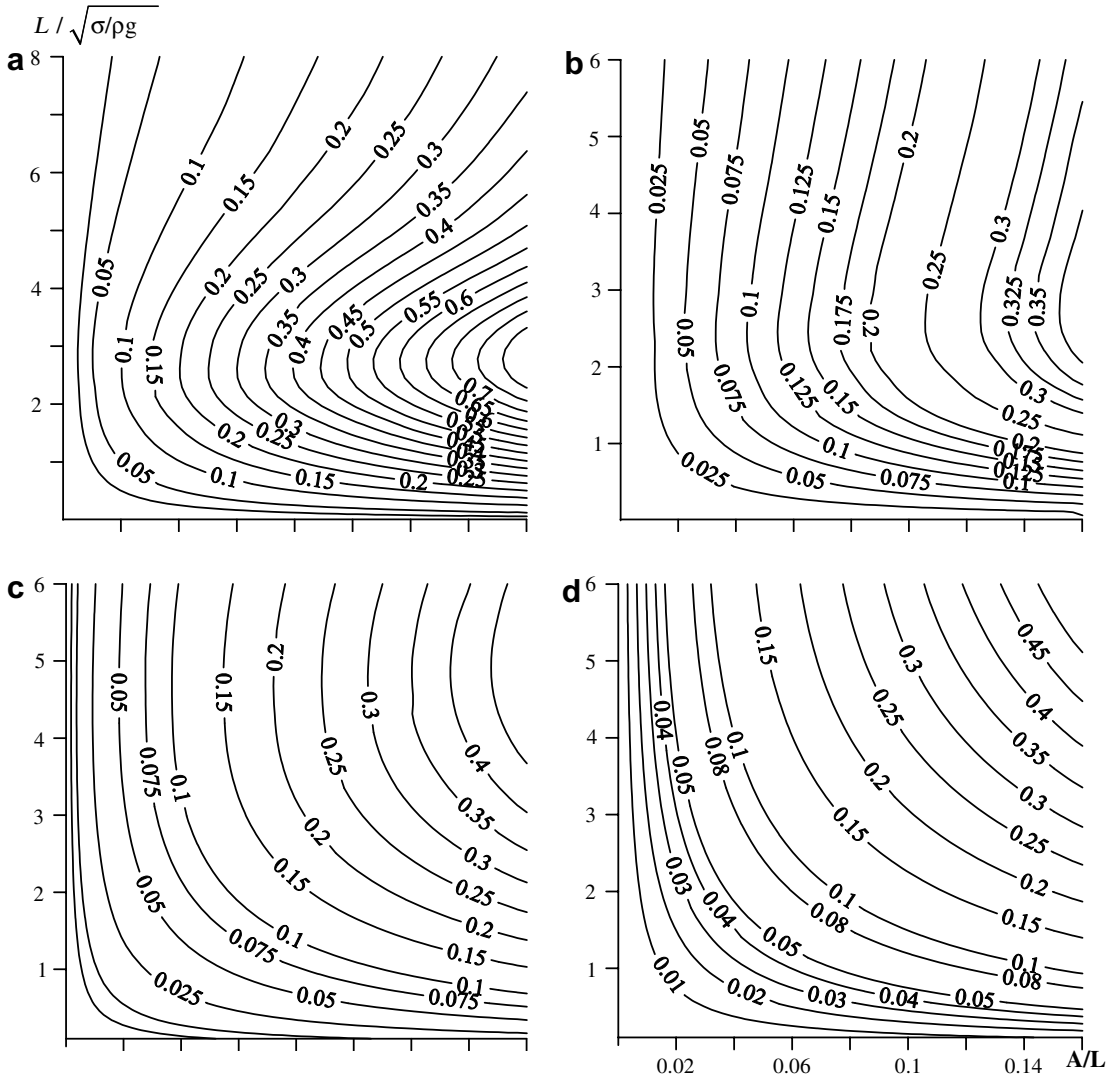

Fig. 11. Contour lines of $(H_{\max} - H_{\min})$ on the plane of the corrugation parameters. Values of $Fi^{1/11} = 2$: (a) corresponds to $Re = 1$; (b) $Re = 5$; (c) $Re = 20$; (d) $Re = 50$.

Line 2 in Figs. 5 and 6 bounds the parameters region where the steady-state solutions are stable with respect to arbitrary disturbances with $Q \in [0, 1]$. At finite values of $Q \neq 1/2$ the spectrum of problem (15) consists of complex eigenvalues. At $Q = 1/2$ the spectrum consists of real eigenvalues and pairs of the complex conjugate eigenvalues. At $Q > 1/2$ the eigenvalues of problem (15) are complex conjugate to the corresponding eigenvalues at $Q_1 = 1 - Q$. Thus, we have a lot of branches of $\lambda_i(Q)$, $i = 1, \ldots, (3M + 1)(N - 1)$. Most of them are with a very large positive value of Real(λ) for all values of $Q \in]0, 0.5]$. Fig. 7 demonstrates two branches of Real(λ) for three steady-state solutions (different periods of corrugation) at constant Ka, Re and A/L. In the spectrum of problem (15) there is the disturbance that demonstrates the vanishing value of Real(λ) with the Q decreasing (branch 1 in Fig. 7). This branch can have positive or negative value of Real(λ) at small Q (the "long-modulated" disturbances) and one controls the stability/unstability of steady-state solution at finite values of Q. Let us emphasize that the "long-modulated" mode has zero value of λ at $Q = 0$ and the parameters regions where all disturbances are stable can be very different from those of where the basic solution is stable with respect to disturbances with $Q = 0$. For example, we did not find solutions which are stable with respect to disturbances with $Q \neq 0$ for $Re = 20$ and 50 at $Ka = 10$, for $Re = 50$ at $Ka = 5$ and for $Re = 1$, 5, 10, 20 and

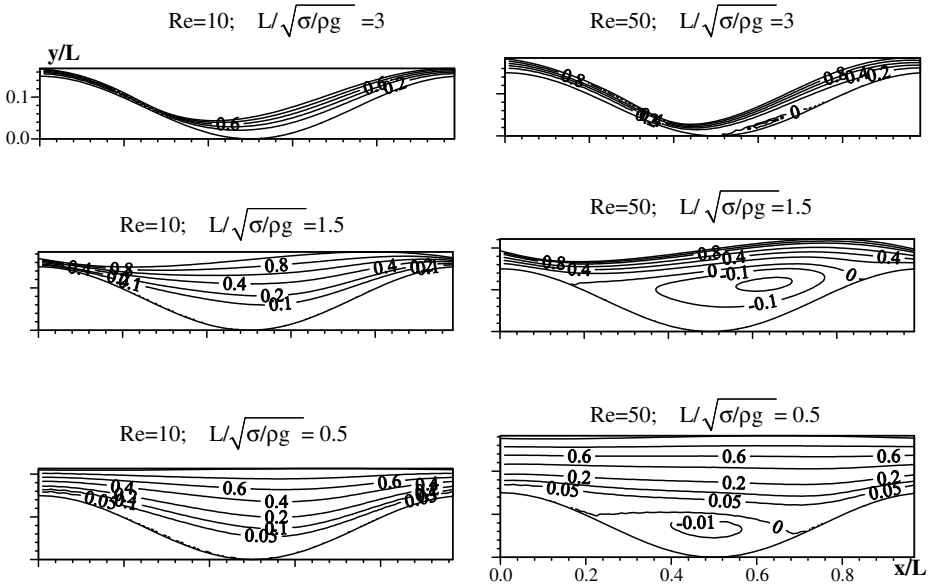

Fig. 12. Contour lines of the streamline function (the fluid particles moves along the lines) and the free surface shape at $Fi^{1/11} = 10$ and $A/L = 0.15$.

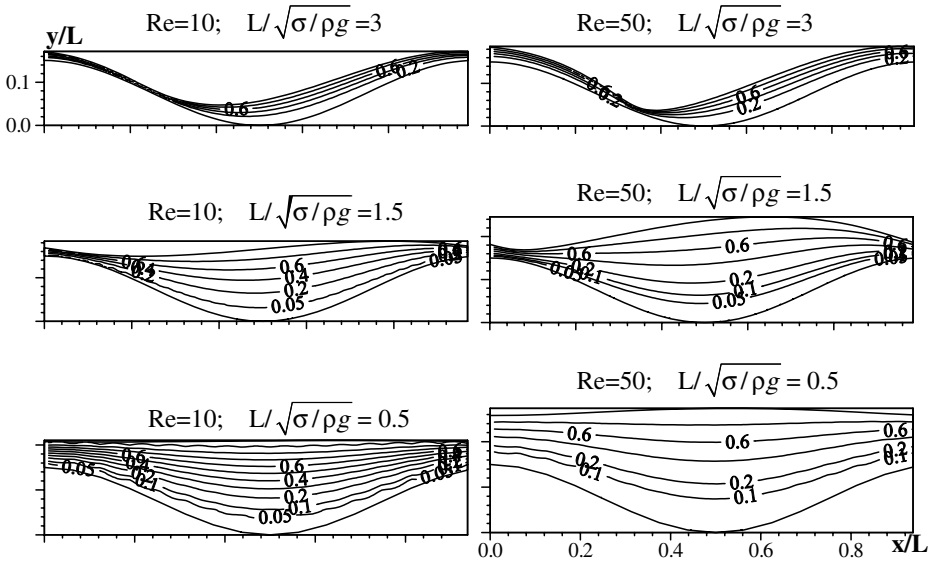

Fig. 13. Integral model. Contour lines of the streamline function and the free surface shape at $Fi^{1/11} = 10$ and $A/L = 0.15$.

50 at $Ka = 2$ inspite of the wide enough region of the parameters where the basic solution is stable with respect to disturbances with $Q = 0$ (see Fig. 4). Let us also note that the integral approach gives good enough description of the stability regions with respect to arbitrary disturbances at $Ka = 10$.

Before the conclusions let us give some additional comments regarding Figs. 12 and 13. In accordance with the Navier–Stokes calculations there is stagnation zone at moderate values of the Reynolds number at some values of the corrugation parameters (it is not possible to have such zones in frame of the integral approach due to suggestion $\partial P/\partial y = 0$ used by the approach). The stagnation zone can exist even for the first type of flowing when the film free surface follows the corrugations shape (see Fig. 12). Negny et al. (2001a,b) observed

such type of flowing with vortex both experimentally and numerically considering the film flow over a wavy wall in cylindrical geometry ($A/L \approx 0.36, Ka \approx 10, L/\sqrt{\sigma/\rho g} \approx 8$). Stagnation zone in their calculations was found starting from small values of $Re \approx 4$. There is no vortex at such small values of Re in our case for these values of the corrugation parameters. There are two finite curvatures of the film free surface in their calculations. First of them is connected with the wavy wall. Second curvature is connected with the cylindrical geometry and one varies over the corrugation period. This variation is comparable with the first curvature changes and it gives new force that is not included in our equations. It will be interesting work to extend our analysis for the cylindrical geometry.

6. Conclusions

Theoretical analysis of linear stability of the viscous liquid film flowing down a wavy surface is carried out. The study is based on the Navier–Stokes equations in their full statement. The developed numerical algorithm allows us to obtain pioneer results in the stability of the film flow down a corrugated surface without asymptotic approximations in a wide range over Reynolds and Kapitsa's numbers. Results presented in the paper allow the following conclusions to be drawn:

- There exist corrugation parameters at which the steady-state solution is unstable with respect to perturbations of the same period as the period of corrugation. In this case the waveless solution cannot be observed in reality and the wall corrugation demonstrates a destabilizing effect. It is obtained that the bound of such instability is close to line $L/\lambda^*_{\text{neut}} = 1$ for all values of the corrugations amplitude considered in the paper (L is the corrugation period, λ^*_{neut} is the length of neutral disturbance for the film flow down a smooth surface). Below this line $\left(L < \lambda^*_{\text{neut}}\right)$ the steady-state solution is stable with respect to perturbations of the same period.
- At the same time, there is a region of the corrugation parameters (amplitude and period) where all perturbations decay in time at moderate values of Reynolds number. In this case the wall corrugation demonstrates a stabilizing effect. At larger values of the Reynolds number there are the "long-modulated" disturbances growing in time. As a result the more complicated regimes of flowing down a corrugated surface can be formed. In frame of the integral approach such regimes were studied by Trifonov (2007). It will be interesting problem in future to consider the wavy regimes of flowing down a corrugated surface by use of the Navier–Stokes equations.
- It is shown that the well-known results of the stability analysis of the film flow down a smooth surface obtained by use of both asymptotic and integral approaches are not valid almost for all Reynolds numbers at small values of the Kapitsa's number and ones are not valid starting from moderate Reynolds numbers at large values of the Kapitsa's number. It is obtained that the wavelength of neutral disturbances becomes be not dependent on the liquid flow rate at large values of Reynolds number.
- It is shown that in the region of the corrugation parameters (period and amplitude) considered in the paper there are two types of flowing down a wavy surface – (a) film free surface follows the wall shape or (b) the film flow demonstrates an area of "thick" film over the corrugation period resulting in an essential increasing of both the averaged film thickness and the difference between the film thickness maximum and minimum. The second type of flowing can be splitted additionally into the flowing with the deformed free surface and with the free surface that is almost parallel to the x-axis. The corrugation parameters of the second regime of flowing are inside the stability zone.
- There is the practically important region of the corrugation and flow parameters ($A/L \leqslant 0.2$, the Nusselt's film thickness is comparable with the corrugations amplitude) where the integral approach gives results which are in good agreement with the corresponding results obtained by use of the Navier–Stokes equations in their full statement.

Acknowledgement

This work was supported by the Russian Foundation for Basic Research, Projects No. 05-08-01238a.

Appendix

$$a_1^1 = \frac{\mathrm{d}}{\mathrm{d}x}\int_0^1 u_b\,\mathrm{d}\eta';\quad a_2^1 = \int_0^1 u_b\,\mathrm{d}\eta';\quad a_3^1 = \frac{\mathrm{d}H_b}{\mathrm{d}x};\quad a_4^1 = H_b;$$

$$a_1^2 = -\frac{\bar\eta_x}{H_b}\frac{\partial P_b}{\partial\eta} + \frac{1}{\varepsilon Re}\left(2\frac{\bar\eta_y^2}{H_b}\frac{\partial^2 u_b}{\partial\eta^2} + \varepsilon^2\left[2\frac{\bar\eta_x^2}{H_b}\frac{\partial^2 u_b}{\partial\eta^2} + 2\frac{\bar\eta_x}{H_b}\frac{\partial^2 u_b}{\partial x\,\partial\eta} + \left(\frac{\bar\eta_{x\xi}}{H_b} + 3\frac{\bar\eta_x\bar\eta_{x\eta}}{H_b}\right)\frac{\partial u_b}{\partial\eta}\right]\right)$$
$$-\frac{\bar\eta_y}{H_b}\frac{\partial(u_b v_b)}{\partial\eta} - \frac{\bar\eta_x}{H_b}\frac{\partial u_b^2}{\partial\eta};$$

$$a_2^2 = -\frac{\eta}{H_b}\frac{\partial P_b}{\partial\eta} + \frac{\varepsilon}{Re}\left[2\frac{\bar\eta_x\eta}{H_b}\frac{\partial^2 u_b}{\partial\eta^2} + 2\frac{\eta}{H_b}\frac{\partial^2 u_b}{\partial x\,\partial\eta} + 2\left(\frac{\bar\eta_{x\eta}\eta}{H_b} + \frac{\bar\eta_x}{H_b}\right)\frac{\partial u_b}{\partial\eta}\right] - \frac{\eta}{H_b}\frac{\partial u_b^2}{\partial\eta};$$

$$a_3^2 = \frac{\varepsilon}{Re}\frac{\eta}{H_b}\frac{\partial u_b}{\partial\eta};\quad a_4^2 = \bar\eta_y\frac{\partial v_b}{\partial\eta} + 2\frac{\partial u_b}{\partial x} + 2\bar\eta_x\frac{\partial u_b}{\partial\eta};\quad a_5^2 = 2u_b;$$

$$a_6^2 = -\frac{\varepsilon}{Re}(\bar\eta_{x\xi} + \bar\eta_x\bar\eta_{x\eta}) + \bar\eta_y v_b + 2\bar\eta_x u_b;\quad a_7^2 = -\frac{\varepsilon}{Re};\quad a_8^2 = -\frac{\varepsilon\bar\eta_x^2}{Re} - \frac{\bar\eta_y^2}{\varepsilon Re};$$

$$a_9^2 = -\frac{2\varepsilon\bar\eta_x}{Re};\quad a_{10}^2 = \bar\eta_y\frac{\partial u_b}{\partial\eta};\quad a_{11}^2 = \bar\eta_y u_b;\quad a_{12}^2 = \bar\eta_x;\quad b_1^2 = -\frac{\eta}{H_b}\frac{\partial u_b}{\partial\eta};$$

$$a_1^4 = (1-K^2)\varepsilon^2\frac{\partial v_b}{\partial x}\bigg|_{\eta=1};\quad K = \varepsilon\left(\frac{\mathrm{d}H_b}{\mathrm{d}x} + \frac{1}{\varepsilon_1}\frac{\mathrm{d}f}{\mathrm{d}x}\right);$$

$$a_2^4 = \left[-(1-K^2)\varepsilon^2\frac{\partial v_b}{\partial\eta} - 2\varepsilon K\left(\frac{\partial u_b}{\partial\eta} + \varepsilon^2 H_b\frac{\partial v_b}{\partial x} - \varepsilon K\frac{\partial v_b}{\partial\eta}\right) + 4\varepsilon^2\frac{\partial v_b}{\partial\eta}\right]\bigg|_{\eta=1};$$

$$a_3^4 = (1-K^2);\quad a_4^4 = (1-K^2)\varepsilon^2 H_b;\quad a_5^4 = -\varepsilon K(1-K^2) + 4\varepsilon K;$$

$$a_1^5 = \frac{\partial}{\partial x}\int_0^\eta u_b\,\mathrm{d}\eta';\quad a_2^5 = \int_0^\eta u_b\,\mathrm{d}\eta' - u_b\eta;\quad a_3^5 = \bar\eta_x H_b;\quad a_4^5 = \frac{\mathrm{d}H_b}{\mathrm{d}x};\quad a_5^5 = H_b;$$

$$a_1^6 = \int_\eta^1\left(-\frac{\bar\eta_y}{H_b}\frac{\partial P_b}{\partial\eta'} + \frac{\varepsilon}{Re}\left(2\frac{\bar\eta_y^2}{H_b}\frac{\partial^2 v_b}{\partial\eta'^2} + \varepsilon^2\left[2\frac{\bar\eta_x^2}{H_b}\frac{\partial^2 v_b}{\partial\eta'^2} + 2\frac{\bar\eta_x}{H_b}\frac{\partial^2 v_b}{\partial x\,\partial\eta'} + \left(\frac{\bar\eta_{x\xi}}{H_b} + 3\frac{\bar\eta_x\bar\eta_{x\eta}}{H_b}\right)\frac{\partial v_b}{\partial\eta'}\right]\right)\right.$$
$$\left. -\frac{\varepsilon^2\bar\eta_y}{H_b}\frac{\partial v_b^2}{\partial\eta'} - \frac{\varepsilon^2\bar\eta_x}{H_b}\frac{\partial(u_b v_b)}{\partial\eta'}\right)\mathrm{d}\eta';$$

$$a_2^6 = \frac{\varepsilon^3}{ReH_b}\int_\eta^1\left[2\bar\eta_x\eta'\frac{\partial^2 v_b}{\partial\eta'^2} + 2\eta'\frac{\partial^2 v_b}{\partial x\,\partial\eta'} + 2(\bar\eta_{x\eta}\eta' + \bar\eta_x)\frac{\partial v_b}{\partial\eta'}\right]\mathrm{d}\eta' - \frac{\varepsilon^2}{H_b}\int_\eta^1\left[\eta'\frac{\partial(u_b v_b)}{\partial\eta'}\right]\mathrm{d}\eta';$$

$$a_3^6 = \frac{\varepsilon^3}{Re}\frac{1}{H_b}\int_\eta^1\eta'\frac{\partial v_b}{\partial\eta'}d\eta';\quad a_4^6 = \varepsilon^2\left(\frac{\partial v_b}{\partial x} + \bar\eta_x\frac{\partial v_b}{\partial\eta}\right);\quad a_5^6 = \varepsilon^2 v_b;\quad a_6^6 = \varepsilon^2\bar\eta_x v_b;$$

$$a_7^6 = \varepsilon^2\left(2\bar\eta_y\frac{\partial v_b}{\partial\eta} + \frac{\partial u_b}{\partial x} + \bar\eta_x\frac{\partial u_b}{\partial\eta}\right);\quad a_8^6 = \varepsilon^2 u_b;$$

$$a_9^6 = -\frac{\varepsilon^3}{Re}(\bar\eta_{x\xi} + \bar\eta_x\bar\eta_{x\eta}) + \varepsilon^2(2\bar\eta_y v_b + \bar\eta_x u_b);\quad a_{10}^6 = -\frac{\varepsilon^3}{Re};$$

$$a_{11}^6 = -\frac{\varepsilon}{Re}\bar\eta_y^2 - \frac{\varepsilon^3}{Re}\bar\eta_x^2;\quad a_{12}^6 = -\frac{2\varepsilon^3}{Re}\bar\eta_x;\quad b_1^6 = -\frac{\varepsilon^2}{H_b}\int_\eta^1\left(\eta'\frac{\partial v_b}{\partial\eta}\right)\mathrm{d}\eta';$$

$$a_1^7 = -\frac{2\varepsilon}{Re}\frac{\bar\eta_y}{H_b}\frac{1+K^2}{1-K^2}\frac{\partial v_b}{\partial\eta}\bigg|_{\eta=1};$$

$$a_2^7 = \frac{3\varepsilon^3 KWe}{(1+K^2)^{5/2}}\left(\frac{\mathrm{d}^2 H_b}{\mathrm{d}x^2} + \frac{1}{\varepsilon_1}\frac{\mathrm{d}^2 f}{\mathrm{d}x^2}\right) + \frac{8\varepsilon^2 K}{Re}\frac{\bar\eta_y}{(1-K^2)^2}\frac{\partial v_b}{\partial\eta}\bigg|_{\eta=1};$$

$$a_3^7 = -\frac{\varepsilon^2 We}{(1+K^2)^{3/2}};\quad a_4^7 = \frac{2\varepsilon}{Re}\bar\eta_y\frac{1+K^2}{1-K^2}.$$

References

Alekseenko, S.V., Nakoryakov, V.E., Pokusaev, B.G., 1992. Wavy Liquid Film Flow, 255. Nauka, Novosibirsk.
Benjamin, T.B., 1957. Wave formation in laminar flow down on inclined plane. J. Fluid Mech. 2, 554–574.
Bontozoglou, V., Papapolymerou, G., 1997. Laminar film flow down a wavy incline. Int. J. Multiphase Flow 1, 69–79.
Chin, R.W., Abernathy, F.H., Bertschy, J.R., 1986. Gravity and shear wave stability of free surface flows. Part 1. Numerical calculations. J. Fluid Mech. 168, 501–513.
DeSantos, J.M., Melli, T.R., Scriven, L.E., 1991. Mechanics of gas–liquid flow in packed-bed contactors. Annu. Rev. Fluid Mech. 23, 233–260.
Fair, J.R., Bravo, J.R., 1990. Distillation columns containing structure packing. Chem. Eng. Prog. 86, 19–29.
Kang, F., Chen, K., 1995. Gravity-driven two-layer flow down a slightly wavy periodic incline at low Reynolds numbers. Int. J. Multiphase Flow 3, 501–513.
Negny, S., Meyer, M., Prevost, M., 2001a. Study of a laminar falling film column: Part I. Numerical investigation of the flow pattern and the coupled heat and mass transfer. Int. J. Heat Mass Transfer 44, 2137–2146.
Negny, S., Meyer, M., Prevost, M., 2001b. Study of a laminar falling film flowing over a wavy wall column: Part II. Experimental validation of hydrodynamic model. Int. J. Heat Mass Transfer 44, 2147–2154.
Nusselt, W., 1916. Die Oberflächenkondensation des Wasserdampfes. Teil I, II. Z. VDI 27, 28, 569–576.
Pozrikidis, C., 1988. The flow of a liquid film along a periodic wall. J. Fluid Mech. 188, 275–300.
Shah, R.K., Focke, W.W., 1988. Plate heat exchangers and their design theory. Heat Transfer Equipment Design. Hemishere, Washington, DC, pp. 227–254.
Shetty, S., Cerro, R.L., 1993. Flow of a thin film over a periodic surface. Int. J. Multiphase Flow 6, 1013–1027.
Trifonov, Yu.Ya., 1998. Viscous liquid film flows over a periodic surface. Int. J. Multiphase Flow 24, 1139–1161.
Trifonov, Yu.Ya., 2004. Viscous film flow down corrugated surfaces. J. Appl. Mech. Tech. Phys. 45, 389–400.
Trifonov, Yu.Ya., 2007. Stability and nonlinear wavy regimes in downward film flows on a corrugated surface. J. Appl. Mech. Tech. Phys. 48, 91–100.
Vlachogiannis, M., Bontozoglou, V., 2002. Experiments on laminar film flow along a periodic wall. J. Fluid Mech. 457, 133–156.
Wang, C.Y., 1981. Liquid film flowing slowly down a wavy incline. AIChE J. 27, 207–212.
Webb, R.L., 1994. Principles of Enhanced Heat Transfer. Wiley, New York.
Wierschem, A., Aksel, N., 2003. Instability of a liquid film flowing down an inclined wavy plane. Physica D 186, 221–237.
Wierschem, A., Lepski, C., Aksel, N., 2005. Effect of long undulated bottoms on thin gravity-driven films. Acta Mech. 179, 41–66.
Zhao, L., Cerro, R.L., 1992. Experimental characterization of viscous film flows over complex surfaces. Int. J. Multiphase Flow 6, 495–516.